# Electronic Supporting Information for Single-Particle ICP-TOFMS with Online Microdroplet Calibration for the Simultaneous Quantification of Diverse Nanoparticles in Complex Matrices

Kamyar Mehrabi[1], Detlef Günther[1], Alexander Gundlach-Graham[1,2]*

1.ETH Zurich, Department of Chemistry and Applied Biosciences, Laboratory of Inorganic Chemistry, Vladimir-Prelog-Weg 1, 8093 Zurich, Switzerland

2. Iowa State University, Department of Chemistry, 2415 Osborne Drive, Ames IA 50011

*Corresponding author: alexgg@iastate.edu

## Table of Contents

**Table S1.** Operating parameters.

| **Microdroplet Introduction** | |
|---|---|
| Droplet Diameter | 65 µm |
| Droplet Frequency | 50 Hz |
| Droplet Burst Length | 1000 droplets, 20 s |
| He Gas Flow in Falling Tube | 0.56 L $min^{-1}$ |
| Ar Gas Flow in Falling Tube | 0.15 L $min^{-1}$ |
| **Pneumatic Nebulizer** | |
| Nebulizer Gas (Ar) | 0.9 L $min^{-1}$ |
| Solution Uptake Rate | ~400 µL $min^{-1}$ |
| **ICP Conditions** | |
| Intermediate Gas Flow (Ar) | 0.8 L $min^{-1}$ |
| Outer Gas Flow (Ar) | 15 L $min^{-1}$ |
| Power | 1550 W |
| Sampling Position | 5.6 mm above load coil |
| **TOFMS Conditions** | |
| TOF Spectral Acquisition Rate | 21.739 kHz |
| Averaged Spectrum Acquisition Rate* | 494.07 Hz (2.02 ms) |

*Averaged mass spectra are composed of data summed from 44 full mass spectra collected every 46 µs.

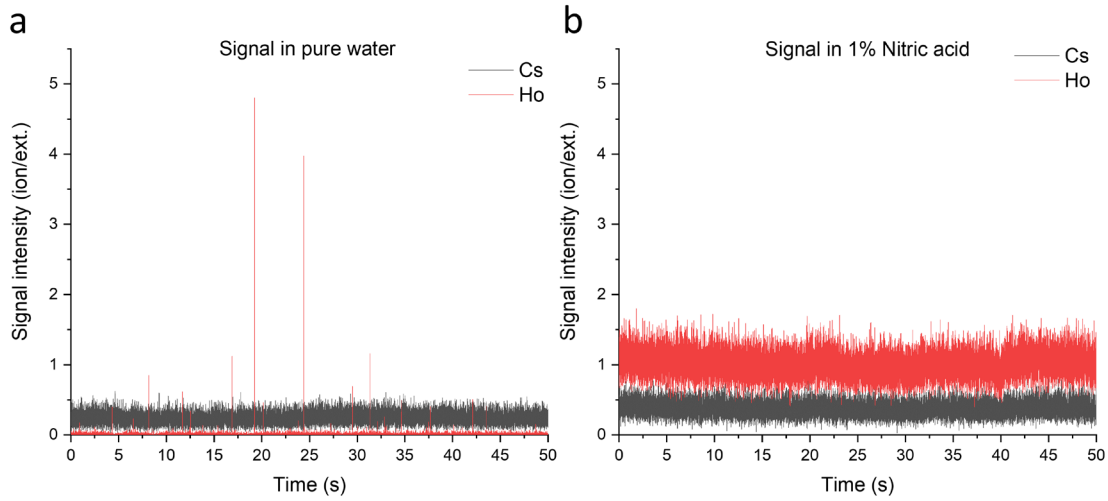


**Fig. S1.** ICP-TOFMS time trace of 5 ng $mL^{-1}$ of Ho and Cs in acid vs. water. Ho signal is spiky in the water sample due to its instability in water. However, Cs signal shows a similar behavior in both samples.

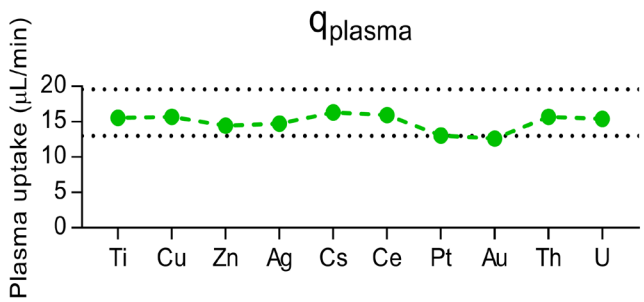


**Fig. S2**. $q_{plasma}$ calculated for several elements using multi-element droplets and dissolved standards of each analyte element. Because a true value of $q_{plasma}$ is not known, all reported values are best estimates. The $q_{plasma}$ determined with Cs, which we use as a plasma-uptake standard, is within 20% (dashed lines) of that obtained for all other elements.

In Fig. S3, we provide results for the quantification of Au NPs in increasing concentrations of Triton X-114 surfactant. Unlike with the PBS buffer (see Fig. 2), we did not observe significant signal attenuation with increasing concentration of Triton, i.e. we did not observe a major plasma-related matrix effect. For Triton matrix, one can size NPs correctly using the conventional particle size method or our online microdroplet method. However, because Triton is a surfactant, it changes the surface tension of the solution and, as a result, it can cause a change in nebulization and transport efficiencies. Increasing Triton concentration causes an increase in the portion of the sample delivered to the plasma. In Fig. S3d, we shown that, by using online plasma-uptake calibration, we are able to measure PNC more accurately and with better consistency (RSD = 7.7%) than if a constant nebulization efficiency were assumed, as is convention in most *sp*-ICP-MS analyses.

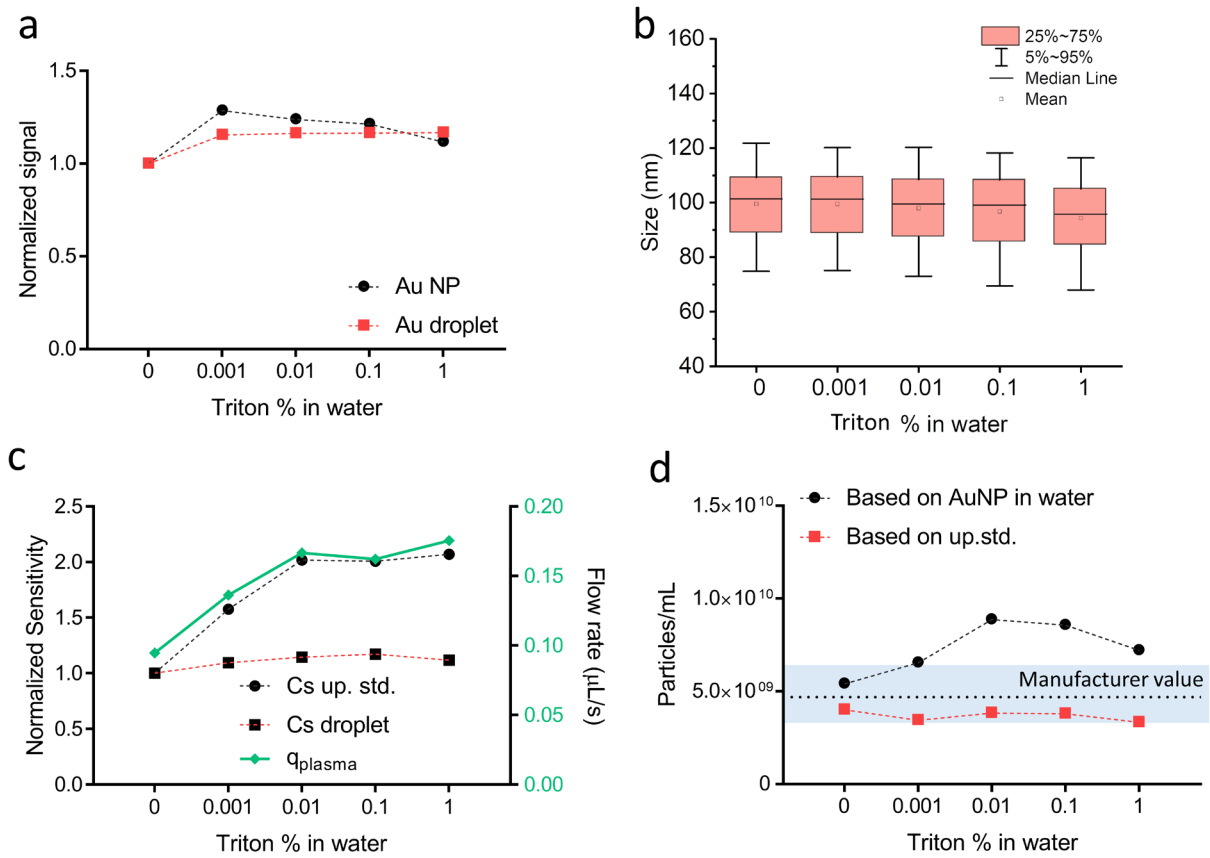


**Fig. S3.** Study on the effect of the matrix on the calibration NP diameter and PNC from a serial dilution of Triton X-114. **a)** Normalized signal intensities from Au in droplets and in NPs for increasing concentrations of Triton. **b)** Determined Au NP diameters in all Triton solutions. The box and whiskers represent the spread of NP diameters determined in three measurement replicates, each of 150 s in duration. **c)** Normalized sensitivities of Cs both from nebulized sample and in microdroplets as a function of Triton concentration and the corresponding $q_{plasma}$ values. **d)** Particle number concentrations of Au NPs based on the conventional particle-size calibration method and with online plasma-uptake determination.

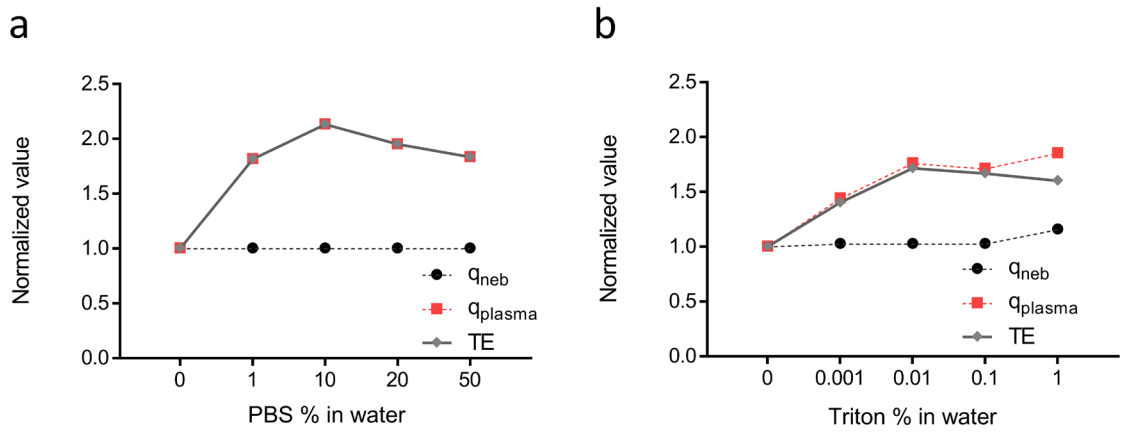


**Fig. S4.** Transport efficiency (TE) determined as $q_{plasma}/q_{neb}$; TE values were normalized to TE in DI water. Liquid flow to the nebulizer was measured online with a liquid flow meter (SLI Liquid Flow Meter, Sensirion, Switzerland). Constant $q_{neb}$ indicates that the changes in $q_{plasma}$ in the PBS (**a**) and Triton-X (**b**) matrices were due to matrix-dependent transport efficiencies.

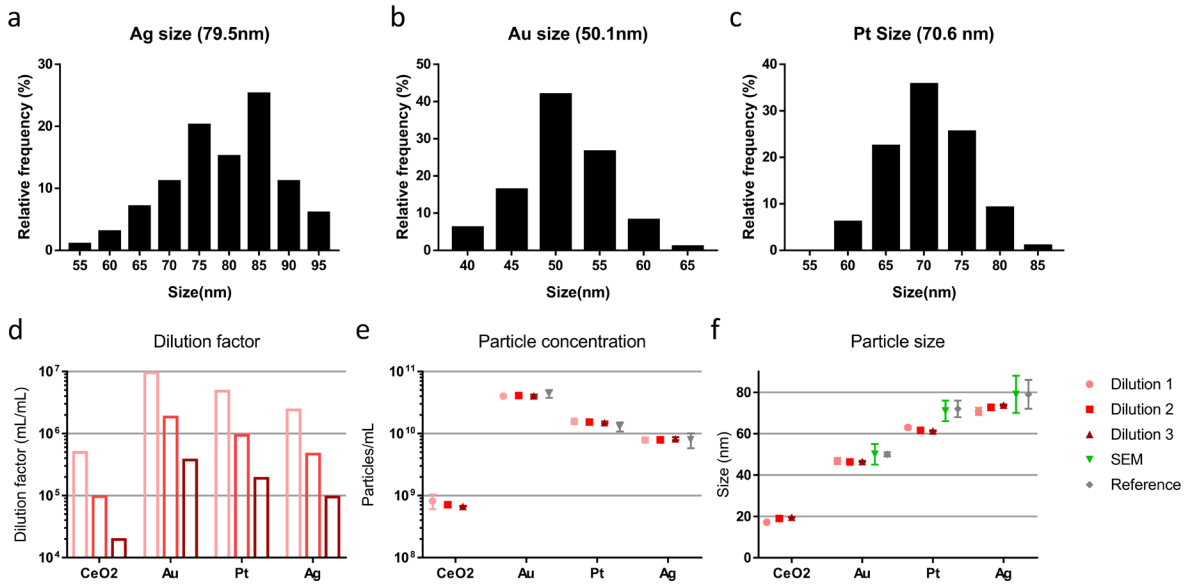


**Fig. S5.** SEM size distribution measurement of silver (**a**), gold (**b**), and platinum (**c**) NPs. Particle number concentrations (**e**) and NP diameters (**f**) for mixtures of NPs in DI water at three dilution factors. In order to have comparable concentrations, measured PNCs in panel (**e**) are back-calculated to the stock concentration; dilution factors of each nanoparticle are provided in (**d**). Good agreement in terms of PNC and NP diameter were found. SEM data representative of sizing which was obtained from SEM and the reference values from manufacturer data sheets.

**Table S2.** LODs, PNCs, and total mass concentrations of NPs found in effluent of WWTP

| Element | Isotope Used | $S_C$* (ion counts) | $X_C$ Mass** (fg) | PNC (particles/mL) | Mass Concentration in NPs (pg/mL)** |
|---|---|---|---|---|---|
| Ti | $^{47}Ti + ^{49}Ti$ | 3.9 | -- | 264 ± 43 | |
| Cr | $^{52}Cr + ^{53}Cr$ | 9.3 | -- | 378 ± 72 | |
| Fe | $^{54}Fe + ^{57}Fe$ | 24 | -- | 396 ± 22 | |
| Mn | $^{55}Mn$ | 12 | -- | 292 ± 58 | |
| Cu | $^{63}Cu + ^{65}Cu$ | 40 | -- | 173 ± 81 | |
| Rh | $^{103}Rh$ | 3.4 | 0.27 | 446 ± 84 | 9.9 ± 4.0 |
| Ag | $^{107}Ag + ^{109}Ag$ | 3.8 | 0.30 | 246 ± 58 | 0.14 ± 0.10 |
| Sn | $^{118}Sn + ^{120}Sn$ | 9.5 | -- | 200 ± 38 | -- |
| La | $^{139}La$ | 4.2 | -- | 68 ± 14 | -- |
| Ce | $^{140}Ce + ^{142}Ce$ | 71 | 2.6 | 16907 ± 337 | 342 ± 33 |
| Pr | $^{141}Pr$ | 3.4 | -- | 209 ± 33 | -- ± |
| Au | $^{197}Au$ | 3.4 | 0.49 | 50 ± 34 | 0.03 ± 0.04 |
| Pb | $^{206}Pb + ^{208}Pb$ | 13 | -- | 246 ± 37 | -- |

*$S_C$ is the signal domain critical value; signals above these count values are considered to originate from particles. This critical value is typically considered to be the limit of detection (LOD) for *sp*-ICP-MS analyses. The critical values used here are based on treating the background as a compound-Poisson distribution[1, 2] and calculated for a false-positive rate of 0.01%. $X_C$ is the content domain critical value, reported in units of mass.
**Mass-based single-particle critical values ($X_C$) and total mass concentration could only be measured for analyte elements that were included in online microdroplet standards, i.e. Ag, Ce, Au, and Pt. The Rh element sensitivity is estimated based on the total-isotope sensitivity of $^{107}Ag+^{109}Ag$.

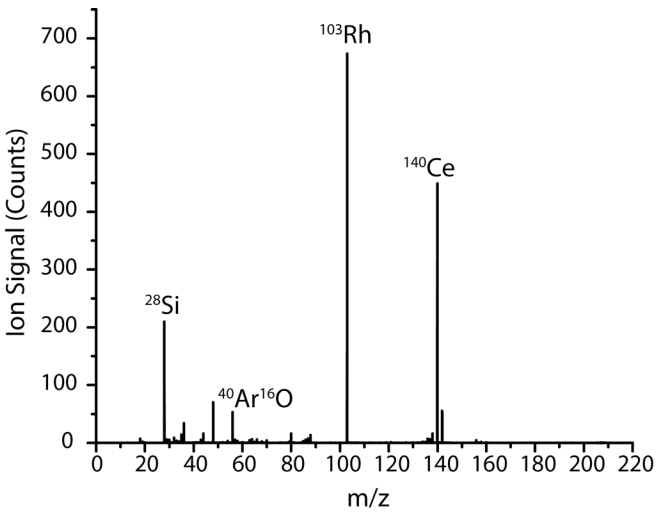


**Figure S6.** Backgroud-subtracted average mass spectrum from 10 $^{103}Rh$-containing particle signals. The absence and/or low abundance of Na, Cu, Sr, and Pb signals from the mass spectrum indicated that potential interfences from $^{23}Na^{40}Ar_2^+$, $^{63}Cu^{40}Ar^+$, $^{87}SrO^+$, and $^{206}Pb^{2+}$ are not responsible for the intense $^{103}Rh^+$ signal. Additionally, the (mono-) isotopic pattern of Rh is observed. Also evident in the average mass spectrum, is the concomitant signal from Ce (measured with the natural ~9:1 isotope ratio of $^{140}Ce$:$^{142}Ce$).

References

1. A. Gundlach-Graham, L. Hendriks, K. Mehrabi and D. Günther, Monte Carlo Simulation of Low-Count Signals in Time-of-Flight Mass Spectrometry and its Application to Single-Particle Detection, *Anal. Chem.*, 2018, **90**, 11847-11855.
2. L. Hendriks, A. Gundlach-Graham and D. Günther, Performance of sp-ICP-TOFMS with signal distributions fitted to a compound Poisson model, *J. Anal. At. Spectrom.*, 2019, **34**, 1900-1909.